Algerian Journal of Environmental Science and Technology
December edition. Vol.9. N°4. (2023)
ISSN : 2437-1114
www.aljest.org

Elaboration of new spherical gelled biocomposites based on ferromagnetic nanoparticles and Al-pillared montmorillonite

A. Hattali [1]*, O. Bouras [2], S. Hanini[1]

[1] Biomaterials and Transport Phenomena Laboratory. Yahia Fares University. Medea 26000. Algeria.
[2] Water Environment and Sustainable Development Laboratory, Blida1 University, BP270-09000, Algeria.

*Corresponding author: ahl_hattali@yahoo.fr; Tel.: +213 697 621 766; Fax: +21325 78 50 80

ARTICLE INFO

Article History :

Received ***: 31/10/2021***
Accepted ***: 05/11/2022***

***Key Words*:**

Adsorption; Encapsulation; Pillared montmorillonite; Ferrofluid; Sodium alginate; gelled beads.

ABSTRACT /RESUME

Abstract: *The main objective of this present work is to develop a new generation of sorbent supports in the form of gelled and hydrophobic magnetic beads based on aluminum-pillared montmorillonite, sodium alginate and magnetic nanoparticles.*
The first step was to prepare the aluminum-pillared montmorillonite as well as the ferrofluid (FF) as a magnetic material. The ferrofluid composed of maghemite nanoparticles (γ-Fe_2O_3) coated with citrate ions, was characterized by the XRD, SEM, FTIR and VSM methods.
The prepared wet biocomposites beads were used in the sorption in a batch system of methyl green (MG). The effects of pH and initial pollutant concentration on the MG removal were investigated. For all the classes of beads prepared, the kinetic study showed that it is the pseudo-first-order model which best describes the behavior of MG towards the sorbent beads. The modeling of sorption isotherms showed that the Sips model gives more satisfactory results than those of Freundlich and Langmuir.

I. Introduction

The use of membranes in water treatment is often confronted with the drawbacks of clogging, storage of sludge resulting from physicochemical and biological treatments and therefore entails a high cost of the nanofiltration process [1,2].
In this context, the use of solid magnetic materials in water treatment could provide solutions of these drawbacks of current methods.
The concept of magnetic separation in depollution consists of adding magnetic particles to the mixture which could adsorb various pollutants (organic or inorganic) and then extracting them by applying a magnetic field gradient.
Researchers are seeking to develop high-performance magnetic adsorbents, which is clear from the number of articles and patents published between 1986 and 1990. In fact, more than 1000 patents and 1900 articles have been published in this field [3].
In 2004 Oliveira et al. [4] added iron oxide to a zeolite for the extraction of metal cations. In 2014, Obeid G. studied the adsorption of methylene blue on magnetic nanoparticles functionalized by citrate ions. The amount of adsorbed methylene blue of the order of 97% was obtained over a wide pH range from 4.2 to 10.3 [1].
D. Talbot et al. (2018) mixed a solution of sodium alginate and ferrofluid to obtain a new magnetic nanocomposite to adsorb methylene blue. The obtained results showed that the adsorption capacity of the dye is higher than 273 $mg.g^{-1}$ [5].
Recently, several types of magnetic materials have been encapsulated with polymers and used in water treatment [6-10].
The modification of clays by intercalation has made it possible to prepare intercalated clays of very diverse natures depending on the nature of the intercalating agents (inorganic metallic polycations, organic polymers, tris-chelate metals, organometallic complexes, etc.) [11.12].

Pillaring by intercalation between the clay sheets of large single or mixed metal polycations allows to obtain microporous materials, with large basal spacing and a very thermally stable structure [13]. Hydrophobic and organophylic organo-inorgano-clay complexes in which organic molecules are co-adsorbed by inorgano-clay complexes are characterized by strong adsorbent properties towards both organic and/or inorganic pollutants [14-2]. In the field of powder shaping, the encapsulation of clay particles in spherical gelled beads has also been very successful in recent years [15-19].
The main objective of this present study is to prepare hydrophobic, magnetic and stable spherical gel beads for the adsorption of Methyl Green dye. This new generation of sorbent gel matrices is synthesized based on aluminum-pillared clay (Al-Mt), Ferrofluid (FF) as a magnetic nanoparticles and sodium alginate (AS).

II. Materials and methods

II.1. Materials

Alginic acid sodium salt $(C_6H_7NaO_6)n$, 99% (Panreac, Quimica SA, high viscosity). Ferric chloride hexahydrate ($FeCl_3$•$6H_2O$), Ferrous chloride dihydrate ($FeCl_2$•$2H_2O$), Ammoniac (NH_4OH), Sodium hydroxide (NaOH), Trisodium citrate ($C_6H_5Na_3O_7$) and HCl were purchased from (PANREAC). Aluminum chloride $Al\boldsymbol{Cl_3}.6\boldsymbol{H_2}O$, 99 % (Acros) and Hydrated iron nitrate ($Fe(NO_3)_3.9H_2O$) were purchased from (BIOCHEM) . Calcium chloride solutions were prepared by dissolving a known amount of $CaCl_2$, $2H_2O$, 98% (PROLABO) in distilled water. Methyl green solutions ($C_{26}H_{33}C_{l2}N_3C_{l2}Zn$) (Cationic dye), with molecular weight= 458.47 $g.mol^{-1}$ and pKa =11,5.

II. 2. Preparation of adsorbents

II. 2.1. Preparation of magnetic nanoparticles (Ferrofluid)

The magnetic material used is a ferrofluid (FF) composed of maghemite (γ-Fe_2O_3) nanoparticles coated with citrate ions. It was prepared under the following conditions:
The particles were synthesized by co-precipitation of a stoichiometric mixture of ferrous and ferric chlorides in an ammonium hydroxide solution. The obtained magnetite precipitate (Fe_3O_4) was acidified with nitric acid and oxidized to maghemite (γ-Fe_2O_3) at 90 ° C with iron (III) nitrate. To obtain a stable magnetic dispersion compatible with the alginate gel (neutral medium), these particles were covered with citrate anions [6,20,21]. After precipitation with acetone, the coated particles were filtered, dried at 40 °C and then ground to obtain a stable magnetic nanoparticle powder designated below as (FF).

II.2.2. Preparation of aluminum-pillared montmorillonite

The used clay comes from a batch of natural bentonite (Maghnia deposit in western Algeria). It is supplied by ENOF (National Company for Useful Substances and Non-Ferrous Products). This bentonite has already been characterized previously by Bouras [22].The preliminary treatment of the bentonite and the recovery of the homoionic sodium fraction (< 2 µm) by sedimentation called "Na-Mt" were previously optimized by Khalaf et al. [23].
The preparation of the pillaring solution providing aluminum hydroxide polymers consists in titrating, using a peristaltic pump, an aluminum chloride solution with 0,225 M caustic soda according to the following conditions previously optimized by Bouras [22]:
Al/Mt-Na = 5 $mmol.g^{-1}$; [Al]f = 0.1 $mol.L^{-1}$; [$AlCl_3.6H_2O$] = 0.5 $mol.L^{-1}$; OH/Al = 1.8; [NaOH] = 0.225 $mol.L^{-1}$; Clay suspension : 0.5 %; Flow = 1.5 $mL.min^{-1}$.
The solution obtained at the end of the titration must be subjected to vigorous stirring for a further period of time in order to ensure complete homogenization. This solution was kept in the dark for maturation for 48 hours.
Suspensions of Na-Mt with concentrations generally equal to 0.5%, initially well homogenized for one hour, are titrated dropwise (8.1 $mL.min^{-1}$) using a peristaltic pump, with the pillaring solution (PCBA) under rapid and permanent agitation. The objective is not only to space the layers of the mineral as much as possible and further widen their basal distances, but also to create pores in the plane of this mineral.
At the end of the titration, the modified montmorillonite was left in contact with the metals polycations for about 4 hours in order to ensure good insertion.

After several washes with distilled water and vacuum filtration, the obtained solids called also inorgano-montmorillonite complexes, are dried at 40 °C for 24 hours. The entire pillared clay preparation protocol is summarized in the Figure 1.

II.2.3. Preparation of biocomposites gelled beads

A viscous and homogeneous solution of sodium alginate (AS) was prepared by gradually adding 1 g of AS (powder) to 100 mL of distilled water under magnetic stirring for 4 hours.

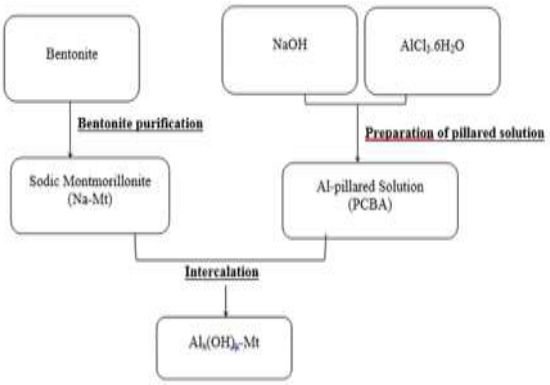

Figure 1. *Flowchart showing the different experimental methods of processing and modifying the used bentonite*

The powdered aluminum pillared clay (Al-Mt) and/or FF masses are then added separately and slowly to the initial sodium alginate solution. All obtained mixtures are kept under rapid stirring for two hours. The obtained homogeneous suspensions are introduced drop by drop using a peristaltic pump with a flow rate 3.3 mL.min^{-1} in a calcium chloride bath (0.1 M; 200 mL)
The gelled beads thus obtained are washed three times with distilled water and with magnetic stirring for 1 hour 30 minutes and then stored in tinted bottles containing distilled water. The compositions of the prepared formulations are summarized in Table 1. Figure 2 illustrates the experimental device for preparing the various biocomposites gelled beads.

Table 1. *Composition of biocomposites gelled beads*

Formulation	AS (g)	Al-Mt (g)	FF (g)
AS/Al-Mt	1	2.5	0
AS/AlMt/FF	1	2.5	0.3

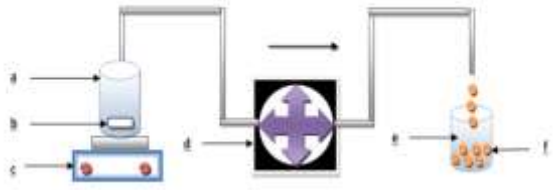

Figure 2*. Diagram of the experimental device illustrating the preparation of the beads.*
(a) Mixture of (AS/Al-Mt) or (AS/Al-Mt/FF); (b) Magnetic bar; (c) Magnetic stirrer; (d) Peristaltic pump; (e) Solution of $CaCl_2$; (f) Gelled beads.

II.3. Characterization of prepared adsorbents

The physical properties of aluminum-pillared montmorillonite have already been determined in previous work [22]. The methods [Vibrating magnetometer (VSM) (MicroSense EasyVsM 20160209-01), X-ray diffractometers (XRD) (Rigaku; SmartLab SE; detector D / TEX U250), Scanning Electron Microscopy (SEM) (QUANTA 250; HV: 20Kv; spot: 3; detector: ETD) and Fourier Transform Infrared Spectroscopy (Frontier FT-IR / Jasco type 4100)] were used for the characterization of magnetic nanoparticles (FF).
The FTIR was also used to determine the spectra of biocomposites gelled beads prepared in the range of 400 – 4000 cm $^{-1}$ using KBr pellets.
The diameter of the prepared beads was determined using a digital caliper.
The water content of the prepared biocomposite gelled beads was determined according to the following equation:

$$\%\, \boldsymbol{W} = \frac{\mathbf{m_H - ms}}{\mathbf{m_H}} * \mathbf{100} \qquad \text{(eq. 1)}$$

Where:
m_H and ms represent the mass of the wet and dry beads, respectively.

The acid-base properties of the prepared beads were determined by potentiometric titration [24]. In each Erlenmeyer flask, 50 mg of adsorbent (biocomposite gelled beads) were added to 50 mL of distilled water for pH varied between 2 and 12. The pH of each solution was adjusted by adding either HCl or NaOH (0.01 M).

II.4. Effect of pH

The pH is an important factor in any adsorption study. It can influence both the surface charge of the sorbent and sorbate. Then, the adsorption test will be depending strongly on the pH value.
For this reason, any study relating to the optimization of the absorption capacity must take into account the behavior of the sorbate as a function of the pH.

In this study, we followed the effect of pH on Methyl Green (MG) adsorption on the two categories of prepared gelled beads:

50 mL of the methyl green solution (C_0 = 10 mg.L^{-1}) is brought into contact with 0.5 g of beads, the pH of the solutions varying between 3 and 9. All the mixtures were prepared at room temperature (20 ± 2 °C) and stirred at 250 rpm with a mechanical stirrer (Edmund Bühler GmbH SM-30).
The pH effect is studied by examining the adsorbed amounts at different pH of these solution mixtures

biocomposite gelled bead/MG. All the solutions obtained after equilibrium are analyzed by UV-Vis spectrophotometry (Pharmaspec Shimadzu (VIS-1700) at the appropriate wavelength λmax (nm) = 626 nm.

II.5. Sorption study

II.5.1. Sorption kinetics

A mass of 0.5 g of each type of prepared biocomposites gelled bead was mixed with 50 mL of an aqueous solution of methyl green (10 mg L^{-1}) with pH equal to 9. The mixtures were prepared at room temperature (20 ± 2 °C) and stir at 250 rpm with a mechanical stirrer (Edmund Bühler GmbH SM-30). Samples are thus taken at different time intervals ranging from 0 to 13 hours.

The MG solutions thus obtained are analyzed by UV-Visible spectrophotometer at the same wavelength of absorption elicited.

The adsorbed quantities (Q_t) and the elimination rate (r) are calculated from the following equations:

$$Q_t = \frac{(C_0 - Ct)}{m} * V \quad \text{(eq. 2)}$$

$$r = \frac{(C_0 - Ce)}{C_0} * 100\% \quad \text{(eq. 3)}$$

With Q_t: Adsorption capacity at time t (in mg g^{-1}); C_0 and C_t: Initial and final concentration of MG (mg L^{-1}); V: Solution volume (L); m: mass of the dried beads (g).

II.5.2. Initial MG concentration effect

Initial concentration effect was studied by analyzing the results obtained from sorption kinetics for different concentrations of methyl green (25, 50, 75 and 100 mg L^{-1}).

II.5.3. Sorption isotherms

Masses of wet gelled biocomposite beads varying from 0.5 to 2.5 mg are mixed with 100 mL of the methyl green solution (C_0 = 10 mg L^{-1}, pH = 9), and stirring at 250 rpm for 3 h.

Sorbed quantities at equilibrium Qe are calculated from the following equation:

$$Qe = \frac{(C_0 - Ce)}{m} * V \quad \text{(eq. 4)}$$

With C_0 and Ce: Initial and equilibrium concentration of MG (mg L^{-1}); V: Solution volume (L); m: mass of the dried beads (g).

III. Results and discussion

III.1. Characterization of the prepared Sorbents

Aluminum pillared montmorillonite (Al-Mt) has already been characterized by Khalaf et al. [23].

The XRD spectrum of the synthesized magnetic nanoparticles was compared to the reference spectrum of maghmite (No. 96-901-2693). The XRD spectrum of the synthesized nanomaterial between the 2θ° confirms that it has a crystal structure of maghmite and all the peaks of γ-Fe_2O_3 (30.29°, 35.71°, 37.35°, 43.28°, 53.81°, 57, 39° and 63.06°) were indexed in the XRD spectrum as shown in Figure 3. Netherless, there are others peaks, can be corresponding to others magnetic components like hematite or magnetite. The average crystallize size D of magnetic nanoparticles was estimated using Scherer's formula [25]:

$$D = \frac{0.9*\lambda}{\beta*\cos\Theta} \quad \text{(eq. 5)}$$

Where θ is the Bragg's angle, λ is the X-ray wavelength and B is the full width at half maximum (FWHM) of the peak, which was determined by Origin.8 software.

The obtained crystallite size of the intense peak (311) is 68.87 nm, and the average crystallite size is around 156.72 nm.

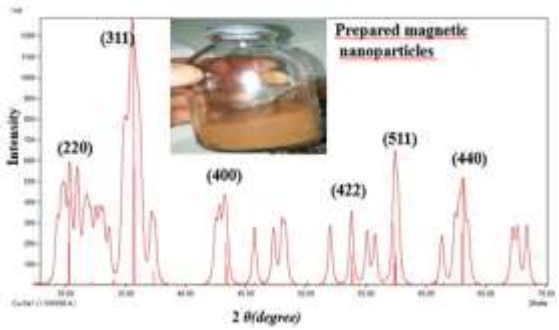

Figure 3*. XRD spectrum of the prepared magnetic nanoparticles.*

Figure 4 shows the magnetic character of the prepared ferrofluids obtained using a vibrating magnetometer at 25 °C, with a magnetic field of up to 22 kOe and a sample vibration of the order of 75 Hz. The results corresponding to these magnetic nanoparticles exhibit superparamagnetic behavior. The saturation magnetization, coercivity and remanence values are of the order of 35.4 emu g^{-1}; 4.90 Oe and 0.21 emu g^{-1}; respectively.

The FTIR spectra of the magnetic nanoparticles prepared from the various studied matrix, which are presented in Figure 5, characterizes the different species grafted to the surface of the nanoparticles and identifies the bonds involved with the surface sites. The obtained spectrum is typical of oxides of

disordered spinel structure, characterized by two wide Fe-O vibrational bands at 636 and 586 cm^{-1}.

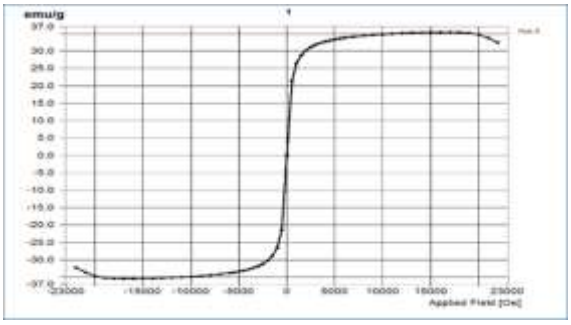

Figure 4. *Magnetic curve of the prepared magnetic nanoparticles.*

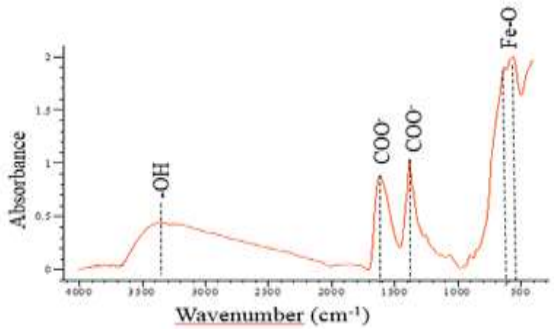

Figure 5. *FTIR spectrum of the prepared magnetic nanoparticles.*

The significant absorbance observed at around approximately 3400 cm^{-1} corresponds to hydroxyl (−OH) stretching bands. The double bands appearing around 1616 cm^{-1} and 1386 cm^{-1} are characteristic of the carboxyl group (COO^{-}) [26].

As shown in Figure 6, SEM analysis shows that the magnetic nanoparticles display an almost spherical geometry, with a non-uniform shape distribution [27].

As shown in Figure 7, the prepared beads are roughly spherical and are whitish in due to the presence of Al-Mt, while those based on FF and Al-Mt are rather brownish.

The average diameter as well as the water content values of the prepared beads are given in Table 2. The corresponding results obtained for the two types of biocomposite gelled beads show good reproducibility.

The magnetic response of the prepared biocomposite gelled beads was tested by placing a neodymium magnet near the glass vial. As shown in Figure 7, these sorbent beads containing FF are attracted to the magnet and can therefore be easily separated from the solution under an external magnetic field.

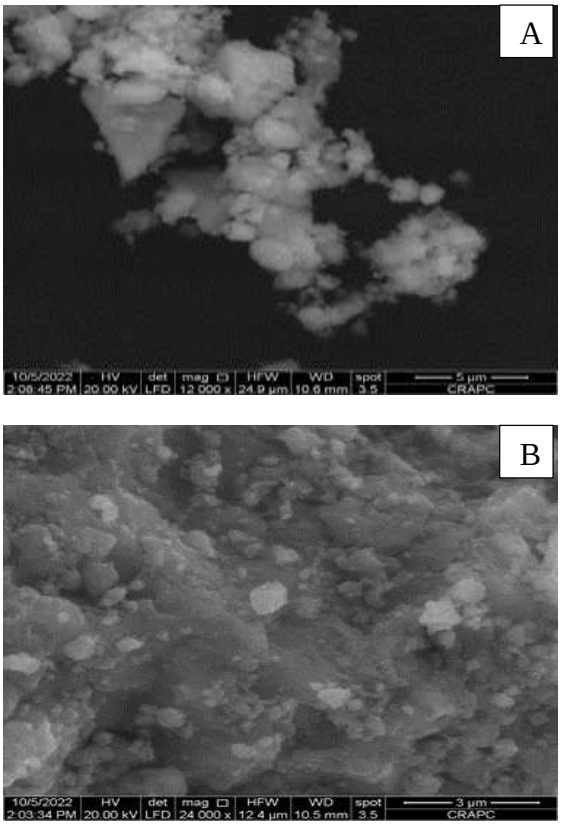

Figure 6. *SEM images of the prepared magnetic nanoparticles. (A) Magnification ×12000, (B) Magnification × 24000.*

Table 2. *Physical characterization of the prepared biocomposites gelled beads.*

Biocomposite gelled beads	**Diameter (mm)**	**Water content (%)**	**pH_{ZPC}**
AS/Al-Mt	3.5	95.08	5.75
AS/Al-Mt/FF	3.5	94.04	6.6

The FTIR spectrum of gelled biocomposite beads shows significant absorbance at around 3400 cm^{-1} corresponding to the characteristic hydroxyl (-OH) stretch bands of alginate. The two bands located at 1635 and 1427cm^{-1} are characteristic of the carboxyl group (COO^{-}). The stretching vibration that peaks around 1036 cm^{-1} and 454 cm^{-1} corresponds respectively to the CO bond and Si-O-Mt characteristic of Al-pillared montmorillonite [16].
The intense absorption band at 529 cm^{-1} in the AS/Al-Mt/FF sample corresponds to the Fe-O

stretching vibration related to the magnetite phase in the prepared magnetic nanoparticles [26].

Figure 7. *Photographies of the prepared biocomposite gelled beads, (A) before and after MG sorption on AS/Al-Mt beads, (B) before and after MG sorption on AS/Al-Mt/FF beads, (C) magnetic separation.*

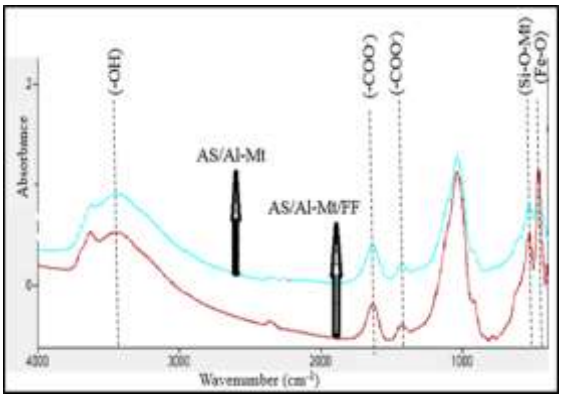

Figure 8. *FTIR spectrum of the prepared biocomposite gelled beads.*

All these results confirm that the Al-Mt and FF powders have been encapsulated with success into sodium alginate matrix and confirm the absence of any reaction between them and sodium alginate.

Figure 9 illustrates the zero charge point (ZCP), where Q is the charge of the adsorbat surface. The pH_{ZCP} values of the prepared beads are given in Table 2. The zero charge point governs the electrophoretic mobility in the sample where the surface charge is neutral.

Potentiometric titration provides a measure of sequential proton binding by surface functional groups of materials [28]. Thus, when the pH of the solution is lower than the pH_{ZCP} of the sorbent, the biocomposite beads would be favorable to the retention of the anionic dye.

On the other hand, when the pH of the solution is higher than the pH_{ZCP} of the sorbent, the surface of the beads becomes negatively charged, and therefore makes it possible to easily sorb the methyl green. Under such conditions, the sorption of methyl green molecules on the biocomposite beads is enhanced due to the electrostatic interaction in the studied pH range.

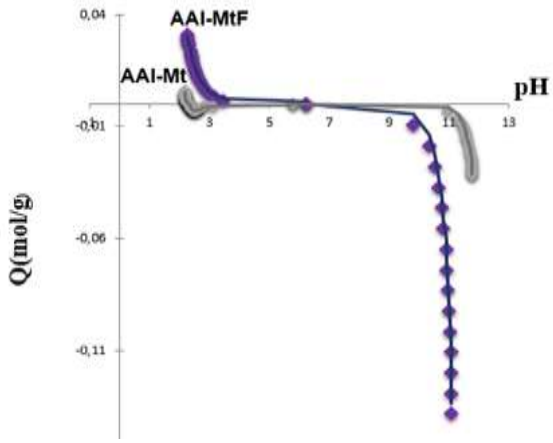

Figure 9. *pH_{zcp} curves for the AS/Al-Mt and AS/Al-Mt/FF biocomposite beads.*

The pH effect on the sorption of the methyl green dye on the two types of prepared biocomposite gelled beads is illustrated in Figure 10. Corresponding results clearly showed that the pH of the solution does not have a significant effect on sorption mechanism of methyl green on the prepared beads in the pH range of 3-9. For the entire pH range studied, the prepared (AS/Al-Mt/FF) and (AS/Al-Mt) beads were found to be effective in sorbing methyl green with removal rates greater than 87 and 89%, respectively.

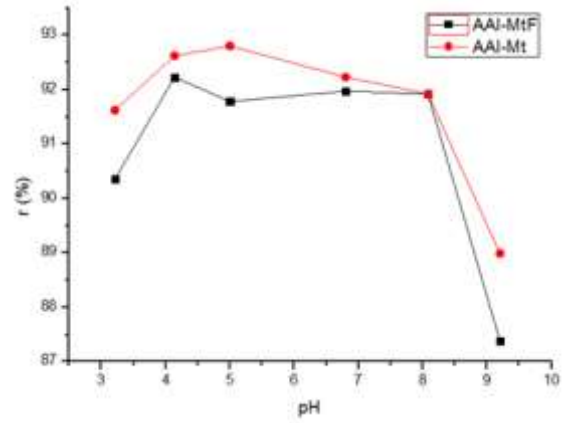

Figure 10. *pH effect concerning methyl green sorption on prepared biocomposite gelled beads (C_0 = 10 mg L^{-1}, t = 4 h, v =250 rpm).*

III. 2. Modelling kinetic sorption

Figure 11 and Table 3 show the results corresponding to the sorption kinetics. These results indicate that the sorption capacity of methyl green increases with the contact time.

The sorption reaches equilibrium after 150 minutes for the two formulations of the biocomposite gelled beads.
The analysis of all these results leads to the conclusion that the the beads of (AS/Al-Mt) and (AS/Al-Mt/FF) types exert almost the same effect for low concentration of methyl green (C = 10 mg L^{-1}).

Table 3. *Data of sorption kinetics of prepared biocomposite gelled beads at pH = 9, C_0 = 10 mg.L^{-1}, T = 28 °C and v =250 rpm*

Biocomposite gelled beads	**MG removal rate r (%)**	**Sorbed quantity Qe (mg g^{-1})**
AS/Al-Mt	88.09	19.06
AS/Al-Mt/FF	89.35	15.94

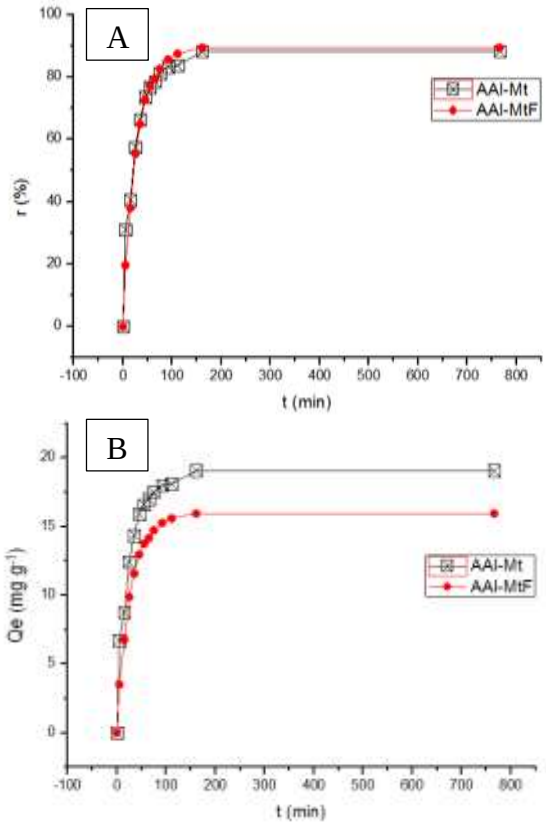

Figure 11*. Sorption Kinetics of MG on the biocomposite gelled beads at pH = 9, C_0=10 mg L^{-1}, T = 28 °C and stirring speed = 250 rpm (A) MG removal Rate (B) Sorbed quantity at equilibrium.*

The experimental results of the sorption kinetics of methyl green on the prepared biocomposite beads were modeled by applying both the pseudo first and pseudo second order kinetic models.

The pseudo first order kinetic model allows us to describe the phenomena that take place during the first minutes of the sorption process. It is described by the following Lagergren equation [29]

$$Q_t = Q_e(1 - e^{-K_1 t}) \qquad \text{(eq. 6)}$$

The linear form of this equation is:

$$\text{Ln}\,(Q_e - Q_t) = \text{Ln}\,(Q_e) - k_1 t \qquad \text{(eq. 7)}$$

Q_e (mg g^{-1}): Sorbed quantity of MG at equilibrium; Q_t (mg g^{-1}): Sorbed quantity of MG at time t; k_1 (min^{-1}): Rate constant kinetic pseudo first order model

The pseudo-second-order equation is often used successfully to describe the reaction kinetics of MG binding to the sorbent [30].

This irreversible model makes it possible to characterize the kinetics sorption by taking into account both the case of solutes rapid fixation at the most reactive sites and that of slow fixation at sites of low energy.

The model of HO and Mckay [31] is a kinetic pseudo second order model. It is defined by the following equation:

$$Q_t = \frac{Q_e^2 K_2 t}{1 + (Q_e K_2 t)} \qquad \text{(eq. 8)}$$

The linear form of this equation is:

$$\frac{t}{Q_t} = \frac{1}{Q_e} t + \frac{1}{K_2 Q_e^2} \qquad \text{(eq. 9)}$$

With Q_e (mg g^{-1}) and Q_t (mg g^{-1}) represent the sorbed quantity of MG at equilibrium; and at time t, respectively; K_2: Rate constant of kinetic pseudo second order model.

The experimental results of sorption kinetics were modeled using both pseudo-first and pseudo-second order models. As shown in Table 4, the kinetic behavior of methyl green sorption on both prepared beads is best described by the pseudo first order model. The correlation coefficients (R^2) are considered to be satisfactory; the calculated Q_e values of the pseudo first order graph are closer to those determined experimentally.

Table 4. *Parameters values related to MG sorption kinetics on the prepared biocomposite gelled beads at pH = 9, T = 28 °C and stirring speed = 250 rpm.*

	Param-eters	**Initial concentration of methyl green (mg L^{-1})**									
		AS/Al-Mt					**AS/Al-Mt/FF**				
		10	**25**	**50**	**75**	**100**	**10**	**25**	**50**	**75**	**100**
	r (**%**)	88.09	94,3	94,98	92,77	86,68	89.35	97,29	97,97	97,24	93,51
	Qe_{exp} (mg g^{-1})	19	47	96	133	184	16	40	81	115	164
Pseudo First Order	Qe_{cal} (mg g^{-1})	18.9	46.9	95.28	132.63	184	15.9	39.65	80.89	114.83	163.41
	K_1 (min^{-1})	0.06	0.03	0.02	0.02	0.04	0.07	0.00	0.01	0.02	0.00
	RMSE	1.46	1.08	0.69	0.81	15.28	1.41	1.72	1.00	0.90	0.52
	R^2	**0.96**	**0.91**	**0.97**	0.86	**0.96**	**1**	0.71	**0.98**	0.77	**0.92**
Pseudo Second Order	Qe_{cal} (mg g^{-1})	18	46.5	46.73	46.95	46.95	15.7	46.3	46.73	46.95	46.3
	K_2 (g $g^{-1}min^{-1}$	1.12	4.90	41.14	60.30	60.65	0.64	2.22	4.03	25.04	2.41
	RMSE	0.03	0.01	0.01	0.01	0.01	0.04	0.04	0.07	0.01	0.01
	R^2	**0.91**	0.81	0.87	0.85	**0.96**	**0.99**	0.17	**0.97**	0.83	**0.99**

The parameters associated with each model were calculated using generic algorithms in MATLAB [32,33].

Initial methyl green concentration effects (25 to 100 mg L^{-1}) on its sorption by the prepared biocomposite gelled beads (AS/Al-Mt) and (AS/Al-Mt/FF) were studied.

As shown in Figure 12, methyl green sorption capacity increases with increasing MG initial concentration. Figure 13 and Table 4 show that (AS/Al-Mt/FF) magnetic biocomposite gelled beads have a higher MG removal rate than AS/Al-Mt beads.

On the other hand, the dye removal rate decreases from 94 to 86% (for AS/Al-Mt beads) when the initial concentration increases. However and for AS/Al-Mt/FF magnetic biocomposite gelled beads, the removal rate remains stable in the order of 97% in the concentration range of 25 to 75 mg L^{-1} but it decreases slightly, and reaches 93% at higher concentration of 100 mg L^{-1}.

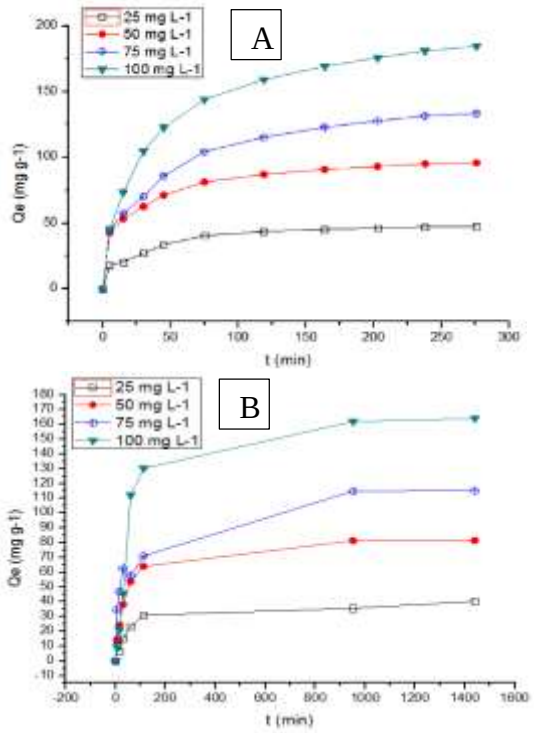

Figure 12. *Initial MG concentration effect on the sorbed quantity at the equilibrium by the prepared beads (A): AS/Al-Mt and (B): AS/Al-Mt/FF (pH = 9, T = 28 °C and v = 250 rpm).*

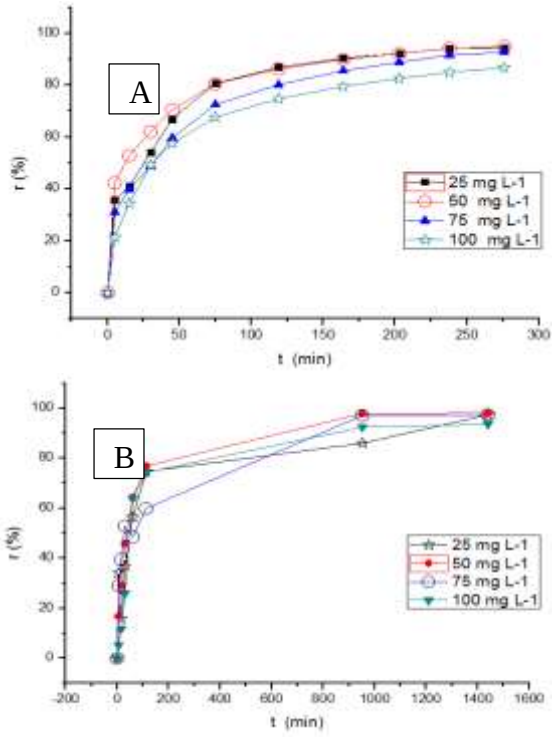

***Figure 13**. Initial MG concentration effect on the dye removal rate by the prepared beads (A): AS/Al-Mt and (B): AS/Al-Mt/FF (pH = 9, T = 28 °C and v = 250 rpm).*

III. 3. Modelling of sorption isotherm

Among the used models, which represent the equilibrium relationship between the sorbed quantity Qe and the concentration of the solute in the solution Ce, the following three classical models can be mentioned:

These are the Langmuir, Freundlich and Sips models.

a. Freundlich Model

Freundlich model is semi empirical. It is based on the assumption of a heterogeneous sorbent surface, with an exponential distribution of active sites as a function of sorption energies [34]. The model equation is written as follows:

$$Qe = Q_m K_F Ce^n \qquad \text{(eq. 10)}$$

With Q_m: Maximum sorption capacity in $mg.g^{-1}$; K_F: Parameter relating to the sorption capacity; n: Parameter relating to the distribution of sorption energies.

The Freundlich parameters are characteristic constants of the couple (sorbent / sorbate), determined experimentally at a given temperature.

However, this model does not admit the existence of a maximum sorption capacity. It is limited to diluted media and only takes into account the (sorbate/sorbent) interactions. The coefficient n is a measure of the sorption intensity or the heterogeneity of the surface. Thus, if n = 1, the partition between the two phases is independent of the concentration. On the other hand, if n < 1, the sorption is quantitatively greater and for n > 1: the intensity of the sorption is lower [34].

b- Langmuir Model

Langmuir model assumes that the surface of the sorbent is homogeneous in terms of energy and does not take into account the interactions between the sorbed molecules [35].

At equilibrium, the Langmuir model equation is given as follows:

$$Qe = \frac{K_L Q_m C_e}{1+K_L C_e} \qquad \text{(eq. 11)}$$

With Q_m: Maximum sorption capacity in $mg.g^{-1}$; K_L: Ratio between sorption and desorption rate constants.

c- Sips Model

Sips proposed a similar equation in form to Freundlich equation, but it has a limit when the concentration is very high [36].

$$Q_e = \frac{Q_m K_s C_e^{ms}}{1+K_s C_e^{ms}} \qquad \text{(eq. 12)}$$

With Ks: Sips equilibrium constant, ms: The exponent of the Sips model.

Figure 14 shows the sorption isotherms of the prepared biocomposite gelled beads. According to the classification established by Giles et al. [37], sorption is described by an L-type isotherm which characterizes a strong attraction between the sorbate and the sorbent. Results show that saturation is not reached but we can still estimate the value of Q_m.

According to Table 5 and Figure 14, the Sips model gives more satisfactory results than the Freundlich and Langmuir models for the two types of prepared biocomposite gelled beads (AS/Al-Mt and AS/Al-Mt/FF).

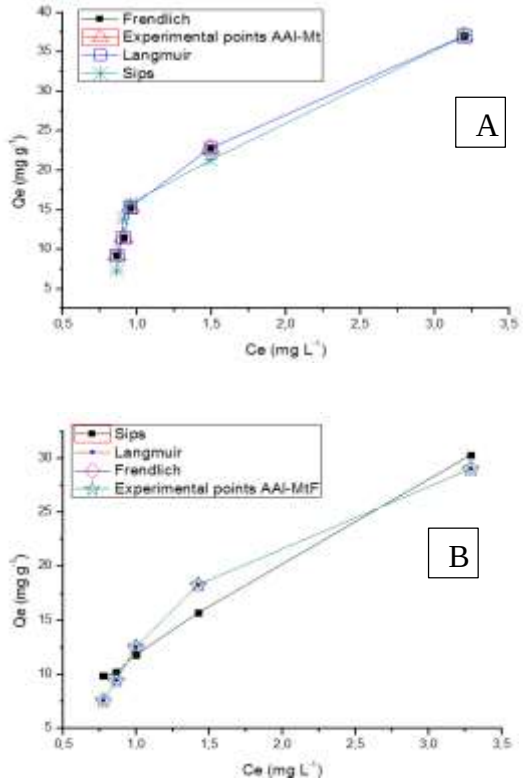

Figure 14. *Modeling of methyl green sorption isotherm (A): AS/Al-Mt beads, (B): AS/Al-Mt/FF beads (t = 1h30, pH = 9, C_0 = 10 mg L^{-1}, T = 28 °C and v = 250 rpm).*

Table 5. *Modeling's constants of methyl green sorption isotherms.*

Mathema-tic Models	**Param -eters**	**AS/Al-Mt**	**AS/Al-Mt/ FF**
Freundlich	K_F	0,41	0.83
	n	0,78	-1.79
	R^2	0,84	0.96
	RMSE	3,97	4.40
Langmuir	Q_m	37	29
	K_L	0.86	0.53
	R^2	0.88	0.95
	RMSE	6.32	3.42
Sips	K_s	0.94	0.44
	ms	9.00	1.82
	R^2	**0.98**	**0.95**
	RMSE	**1.56**	**1.71**

IV. Conclusion

A new generation of sorbent supports in the form of hydrophobic and magnetic gelled beads has been developed and subsequently used in the sorption of methyl green in discontinuous systems.

The two types of biocomposite gelled beads obtained are spherical with a diameter equal to 3.5 mm. Their water content and pH_{zcp} are successively (95%; 5.75) and (94%; 6.6) for AS/Al-Mt and AS/Al-Mt/FF. The pH solution did not have a significant effect on methyl green sorption mechanism on prepared beads in the pH range 3-9. In addition, the sorption capacity increases with the increase of the initial MG concentration and the MG removal rate remains stable for the magnetic biocomposite gelled beads (AS/Al-Mt/FF) (97%) in the range of initial dye concentration [25-75 mg L^{-1}]. The behavior of methyl green sorption kinetics on all the prepared beads is better described by the pseudo first order than that of the pseudo second order model. Regarding the modeling of sorption isotherms, the Sips model gave more satisfactory results than those of Freundlich and Langmuir models.

V. References

1. Obeid, L. Synthèse et caractérisation de matériaux magnétiques pour l'adsorption de polluants présents dans les eaux. Chimie organique. Université Pierre et Marie Curie - Paris VI, 2014. Français.
2. Yano, J. Application of HGMS for water treatment in steel industry. *Industrial Applications of Magnetic Separation* 78 (1979) 134.
3. Fauconnier, N.; Bee, A.; Roger, J.; Pons, J. N. Adsorption of gluconic and citric acids on maghemite particles in aqueous medium. *Progress in Colloid & Polymer Science* 100 (1996) 212.
4. Oliveiraa, L.C.A.; Petkowiczb, D.I.; Smaniottob, A.; Pergherb, S.B.C. Magnetic zeolites: a new adsorbent for removal of metallic contaminants from water. *Water Research* 38 (2004) 3699.
5. Talbot, D.; Abramson, S. pH-sensitive magnetic alginate/γ-Fe_2O_3 nanoparticles for adsorption/ desorption of a cationic dye from water. *Journal of Water Process Engineering* 25 (2018) 301-308.
6. Rocher, V.; Siaugue, J. M.; Cabuil, V.; Bee, A. Removal of organic dyes by magnetic alginate beads. *Water Research* 42 (2008) 1290–1298.
7. Zhang, H.; Omer, A. M.; Hu, Z.; Yang, L.; Ji, C.; Ouyang, X. K. Fabrication of magnetic bentonite/Carboxymethyl chitosan/sodium alginate hydrogel beads for Cu(II) adsorption. *International Journal of Biological Macromolecules* 135(2019) 490-500.
8. Zou, M. F.; Chen, X. Y.; Lin, X. J.; Chen, M. Y.; Ding, N. N.; Yang, L. Y.; Ouyang, X. Fabrication of magnetic carboxyl functionalized attapulgite, calcium alginate beads for lead ion removal from aqueous solutions. *International Journal of Biological Macromolecules* 130 (2018) 789-800.
9. Bee, A.; Talbot, D.; Abramson, S.; Dupuis, V. Magnetic Alginate beads for Pb (II) ions removal from wastewater. *Journal of Colloid and Interface Science* 362(2) (2011) 486-492.
10. Gopalakannan, V.; Viswanathan, N. Synthesis of magnetic alginate hydrid beads for efficient chromium (VI) removal. *International Journal of Biological Macromolecules* 72(2015) 862-867.
11. Akçay, M.; Akçay, G. The removal of phenolic compounds from aqueous solutions by organophilic bentonite. *Journal of Hazardous Materials* 113(1-3) (2004)189-193.

12. Shen, Y. H. Phenol sorption by organo clays having different charge characteristics. *Colloids and Surfaces A: Physicochemical and Engineering Aspects* 232(2-3) (2004) 143-149.
13. Zhao, L. Développement et mise en œuvre de nouveaux matériaux adsorbants d'anions à base de ferrihydrite ou d'Hydroxydes Doubles Lamellaires intégrés dans un gel d'alginate. Université de Limoges (2016) Français.
14. Bouras, O.; Chami, T.; Houari, M.; Khalaf, H.; Bollinger, J.C.; Baudu, M. Removal of sulfacid brillant pink from an aqueous stream by adsorption onto surfactant –modified Ti-pillared montmorillonite. *Environmental Technology* (2001) 405-411.
15. Unuabonah, E. I.; Taubert, A. Clay–polymer nanocomposites (CPNs): Adsorbents of the future for water treatment. *Applied Clay Science* 99 (2014) 83–92.
16. Lezehari, M.; Basly, J. P.; Baudu, M.; Bouras, O. Alginate encapsulated pillared clays: removal of a neutral/anionic biocide (pentachlorophenol) and a cationic dye (safranine) from aqueous solutions. *Journal of Colloids and Surfaces A: Physicochemical and Engineering Aspects* 366 (2010) 88–94.
17. Chabane, L.; Cheknane, B.; Zermane, F.; Bouras, O.; Baudu, M. Synthesis and characterization of reinforced hybrid porous beads: Application to the adsorption of malachite green in aqueous solution. *Chemical Engineering Research and Design* 120 (2017) 291–302.
18. Boukhalfa, N.; Boutahala, M.; Djebri, N.; Idris, A. Kinetics thermodynamic, equilibrium isotherms, and reusability of cationic dye adsorption by magnetic alginate/oxidized multiwalled carbon nanotubes composites. *International Journal of Biological Macromolecules* 123 (2019) 539-548.
19. Song, Y.; Wang, S.; Yang, L. Y.; Yu, D.; Wang, Y. G. Ouyang X k, Facile fabrication of core–shell/bead-like ethylene diamine functionalized Al-pillared montmorillonite/calcium alginate for As(V) ion adsorption. *International Journal of Biological Macromolecules* 131 (2019) 971–979.
20. Fauconnier, N.; Bde, A.; Roger, J.; Pons, J. N. Synthesis of aqueous magnetic liquids complexation of maghemite nanoparticles by surface. *Journal of Molecular Liquids* 83 (1999) 233-242.
21. Massart, R. Preparation of aqueous magnetic liquids in alkaline and acidic media. *IEEE Transactions on Magnetics* 17 (1981) Issue: 2.
22. Bouras, O. Propriétés adsorbantes d'argiles pontées organophiles : Synthèse et caractérisation, thèse de doctorat, université de Limoges N° d'ordre : 02 – 2003 (2003).
23. Khalaf, H.; Bouras, O.; Perrichon, V. Synthesis and characterization of Al-pillared and cationic surfactant modified Al-pillared Algerian bentonite. *Microporous Materials* 8 (1997) 141-150.
24. Chen, J. H.; Ni, J. C.; Liu, Q. L.; Li, S. X. Adsorption behavior of Cd(II) ions on humic acid-immobilized sodium alginate and hydroxyl ethyl cellulose blending porous composite membrane adsorbent. *Desalination* 285 (2012) 54–61.
25. Attaf, A.; Bouhdjer, A.; Saidi, H.; Aida, M. S.; Attaf, N.; Ezzaouia, H. On tuning the preferential crystalline orientation of spray pyrolysis deposited indium oxide thin films. *Thin Solid Films* 625 (2017) 177–179.
26. Mahdavi, M.; Bin Ahmad, M.; Haron, M. J.; Namvar, F.; Nadi, B.; Abd Rahman, M. Z.; Amin, J. Synthesis, Surface Modification and Characterisation of Biocompatible Magnetic Iron Oxide Nanoparticles for Biomedical Applications. *Molecules* 18(7) (2013) 7533–7548.
27. Scherer, C.; Figueiredo Neto, A. M. Ferrofluids: Properties and Applications. *Brazilian Journal of Physics* 35(3A) (2005).
28. Su, C. Environmental implications and applications of engineered nanoscale magnetite and its hybrid nanocomposites: a review of recent literature. *Journal of Hazardous Materials* 322 (2017) 48–84.
29. Lagergren, S. Zur theorie der sogenannten adsorption geioster stoffe. Kunglinga Svenska Vetenskapsakademiens. *Handlingar* 24 (1898) 1-39.
30. Ho, Y. S.; Mckay, G. A comparison of chemisorption kinetic models applied to pollutant removal on various sorbents. *Process Safety and Environmental Protection* 76 B (1998) 332-340.
31. Ho, Y. S., Mckay, G. Pseudo-second order model for sorption processes. *Process Biochemistry* 34 (1999) 451-465.
32. Sediri, M.; Hanini, S. ; Laidi, M. ; Turki, S.A. ; Cherifi, H. ; Mabrouk, H. Artificial Neural Networks Modeling of Dynamic Adsorption From Aqueous Solution. *Moroccan Journal of Chemistry* 5 (2) 236-243.
33. Adda, A.; Hanini, S.; Abbas, M.; Sediri, M. Novel adsorption model of filtration process in polycarbonate track-etched membrane: Comparative study. *Environmental Engineering Research* 25 (2020) 479-487.
34. Ferrandon, F. ; Bouabane, H.; Mazet, M. Contribution à l'étude de la validité de différents modèles, utilisés lors de l'adsorption de solutés sur charbon actif. *Revue des sciences de l'eau* 8 (1995) 183-200.
35. Mansur, H. S.; Sadahira, C. M.; Souza, A. N.; Mansur, A. A. P. FTIR Spectroscopy Characterization of Poly(vinyl alcohol) Hydrogel with Different Hydrolysis Degree and Chemically Crosslinked with Glutaraldehyde. *Materials Science and Engineering: C* 28 (2008) 539-548.
36. Bouarouri, K.; Naceur, M. W.; Hanini, S.; Soukane, S.; Laidi, M.; Drouiche, N. Adsorption of humic acid from seawater on organo Mg-Fe-layered double hydroxides: isotherm, kinetic modeling and ionic strength. *Desalination and Water Treatment* 195 (2020)114-127.
37. 37. Giles, C. H.; MacEwan, T. H.; Nakhwa, S. N.; Smith, D. Studies in adsorption. Part XI. A system of classification of solution adsorption isotherms, and its use in diagnosis of adsorption mechanisms and in measurement of specific surface areas of solids. *Journal of Chemical Society* 786 (1960) 3973-3993.

Please cite this Article as:
Hattali A., Bouras O., Hanini S. Elaboration of new spherical gelled biocomposites based on ferromagnetic nanoparticles and Al-pillared montmorillonite, ***Algerian J. Env. Sc. Technology***, **9:4 (2023) 3353-3363**